Microphytobenthos as a source of labile organic matter for denitrifying microbes

J. Morelle, C. Roose-Amsaleg, A.M. Laverman

Title: Microphytobenthos as a source of labile organic matter for denitrifying microbes

Authors: Jérôme Morelle*, Céline Roose-Amsaleg, and Anniet M. Laverman

Authors affiliation:

Université de Rennes 1, CNRS, ECOBIO [(Ecosystèmes, biodiversité, évolution)] - UMR 6553, Rennes, France

*Corresponding author: jerome.morelle@univ-rennes1.fr

Graphical abstract:

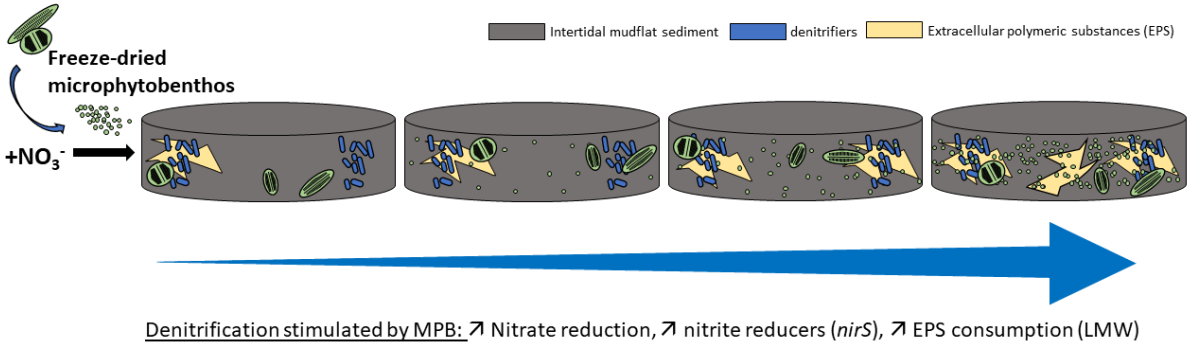

Abstract:

Nitrogen loads in natural waters remain elevated in populated and agricultural areas with serious impact on estuarine and coastal ecosystems. Intertidal sediments can play a significant role in attenuating the high nitrogen levels in water via microbial nitrate reduction, in general dominated by denitrification. These heterotrophic processes are heavily mediated by both the quantity and quality of organic matter available. Benthic microalgae were experimentally investigated as organic carbon source for denitrifying microbes in intertidal mudflat sediments from the Seine Estuary (France). Dry microphytobenthos (including algae and their extracellular polymeric substances) were added to sediments and nitrate reduction rates were monitored over a two-week period using anoxic controlled flow-through reactor approach. Our results show that microphytobenthos addition resulted in significantly higher nitrate reduction (67 to 332% increase), highly related to the added amount of microphytobenthos. Moreover, increase of the low molecular weight carbohydrates consumption (11 to 39%) highlight the measurable contribution of extracellular polymeric substances to the carbon consumption during nitrate reduction. The addition of microphytobenthos increased the abundance of nitrite reductase genes, especially those encoding the *nirS* gene (43 to 152% increase) while nitrous oxide reductase genes (*nosZ* gene) remained constant. Microphytobenthos appeared to favor complete denitrification as suggested by an increase in *nirS* and a decrease in clade II *nosZ* gene copy numbers. This study confirms experimentally the assumption that microbes use microalgae and particularly labile

extracellular polymeric substances as a carbon substrate for nitrate reduction. These results reinforce the impact played by microphytobenthos in intertidal mudflats by highlighting their role on denitrifying microbes and nitrate removal from water.

Keywords:
Microphytobenthos; Nitrate reduction rates; denitrifying microbes; intertidal sediment; extracellular polymeric substances.

1. Introduction

Estuaries cover less than 0.35 % of Earth's surface (Costanza et al. 1997), but are some of the most productive ecosystems (Geider et al. 2001). The stability and long-term management of estuarine ecosystems are threatened by anthropogenic pressure, particularly nutrient loading (Erisman et al. 2008; Barbier et al. 2011; Porter et al. 2013; Zhang et al. 2021). This often leads to undesirable and widespread disturbances such as harmful algal blooms or altered food web dynamics (Le Moal et al. 2019). Whereas phosphorus inputs significantly decreased since the 70s due to improvement of waste water treatment (Liu et al. 2008), nitrogen pollution remains elevated in populated and agricultural areas (Grizzetti et al. 2011; Ukaogo et al. 2020; Zhang et al. 2021). These differences lead to an imbalance in stoichiometric ratios of nitrogen and phosphorous, impacting autotrophic communities, decreasing overall biodiversity and consequently primary and secondary productivity in estuarine and coastal ecosystems (Hillebrand et al. 2014). Many key services, essential for regulation and support of estuarine systems, are provided by shallow water habitats such as salt marshes and mudflats (Jacobs et al. 2013; Mandal et al. 2021). Intertidal mudflats sequester organic carbon (Jickells and Rae 2005), recycle nutrients, contribute widely to the autochthonous estuarine primary production by benthic microalgal assemblages, known as microphytobenthos (MPB), providing nutrition to countless resident and migrating animals (Mayor et al. 2018; Passarelli et al. 2018; Hope et al. 2020). For decades, the role of intertidal sediments in attenuating the high nitrogen loads in estuaries has been studied (Trimmer et al. 1998; Magalhães et al. 2002; Wang et al. 2009; Wadnerkar et al. 2019). However, due to intense hydrodynamics and anthropogenic disturbances such as artificialization of banks, port and town extensions, construction of roads and bridges and sediment removal, reduce mudflat areas and could thus limit these key services (Lesourd et al. 2001, 2016). Especially since, in the context of climate warming, the ecological values of mudflats are also threatened by the upcoming increase in extreme climatic events and sea level rise (van der Wegen et al. 2017).

The removal of nitrogen in intertidal estuarine sediments, mainly performed by microorganisms, can be attributed to several distinct nitrogen transforming processes. Among them, denitrification (Tiedje et al. 1983) and anaerobic ammonium oxidation (anammox, Van de Graaf et al. 1995; Strous et al. 1999; Kuenen 2008) allow inorganic nitrogen reduction into inert N_2 gas, completely eliminating nitrogen from the system. In comparison, dissimilatory nitrate reduction to ammonium (DNRA, Tiedje

1988; Decleyre et al. 2015a) transforms nitrate (NO_3^-) into ammonium (NH_4^+), retaining inorganic nitrogen in the system. These nitrogen transformations occur in anoxic environments in the presence of NO_3^-. Whereas anammox is an autotrophic process, DNRA and denitrification are heterotrophic processes for which the carbon quantity (Starr and Gillham 1993) and quality (Hume et al. 2002; Sirivedhin and Gray 2006; Dodla et al. 2008; Stelzer et al. 2014) in the sediment plays an important role. Processes allowing a complete reduction of inorganic nitrogen into N_2 are especially important since they avoid retention of inorganic nitrogen in systems. Overall, denitrification in coastal sediments has been shown to be dominate over anammox (Zhou et al. 2014). It has been estimated that almost 50% of the nitrogen that enters streams and rivers is denitrified within the estuary before it reaches the coast (Galloway et al. 2004). Denitrification is performed in 4 sequential reactions from NO_3^- to N_2 with nitrite (NO_2^-), nitric oxide (NO) and nitrous oxide (N_2O) as intermediates. The first, NO_3^- reduction, is not specific to denitrification and can be carried out by a wide range of microorganisms. The second, NO_2^- reduction to NO is only performed by denitrifying microbes (Zumft 1997). This reaction is catalyzed by two different types of NO_2^- reductases encoded by the *nirS* or *nirK* genes (for a review see Kuypers et al. 2018). The final step of denitrification allows reduction of N_2O, a powerful greenhouse gas which is catalyzed by the nitrous oxide reductase encoded by the *nosZ* gene (Scala and Kerkhof 1998; Rich et al. 2003; Rösch and Bothe 2009).

The impact of carbon quality related to vegetation type on denitrification has been demonstrated in wetland and mangrove sediments (Bastviken et al. 2007; Fernandes et al. 2016). In intertidal areas, carbon sources are characterized by a large variability in composition and degradability, with terrestrial plants and macrophyte carbon that are more recalcitrant than labile sources such as MPB (Bouillon and Boschker 2006). The role of MPB in nitrogen turnover has been studied and demonstrated with laboratory incubations of natural sediments (Sundbäck and Miles 2002; Tobias et al. 2003), benthic chamber measurements in the field (Eyre et al. 2013), *in situ* ^{15}N pulse-chase experiments (Eyre et al. 2016) or pyrosequencing and qPCR (Decleyre et al. 2015b). Additionally, MPB assemblages produce extracellular polymeric substances (EPS), to facilitate their vertical migration and sediment adhesion, which are highly labile (De Brouwer et al. 2006; Shnyukova and Zolotareva 2017). It was hypothesized that microbes preferentially use EPS as carbon sources (Bouillon and Boschker 2006; Bellinger et al. 2009; Taylor et al. 2013). Whereas these studies highlighted the important role of MPB for N assimilation and as organic carbon source for NO_3^- reduction processes, the cumulative N-assimilation and N-reduction processes did not allow the exact quantification of the MPB's role as organic carbon source for each specific process. The addition of organic carbon in the form of MPB was shown to stimulate NO_3^- reduction rates and modify the denitrifying community composition (Decleyre et al. 2015b; Babbin et al. 2016). In order to specifically determine the role of organic carbon originating from MPB on denitrification, an experimental approach is required controlling processes like photosynthesis or nitrification that can in turn influence denitrification (Bartoli et al. 2021).

In this context, the aim of the present study was to experimentally quantify the impact of MPB and the associated carbon (EPS) on the anoxic NO_3^- reduction processes. Therefore, varying quantities of MPB biomass were added to estuarine sediment sampled in an intertidal mudflat of the Seine estuary and the efficiency of microbial NO_3^- reduction was studied in anoxic and dark conditions by using flow-through reactors (Laverman et al. 2006). In addition to rate measurements, the abundance of key denitrifying genes was determined (*nirK*/*nirS* and *nosZ*) to estimate the role of MPB addition on the denitrifier community. We hypothesized that a higher availability of labile carbon from MPB increases NO_3^- reduction rates and enhances growth of microbes involved in the denitrification process.

2. Material and methods

2.1. Study site and sampling

The Seine estuary is a typical example of elevated riverine nutrient fluxes from the Parisian megapole resulting in eutrophication on the English Channel coast (Billen and Garnier 2007; Billen et al. 2007; Morelle 2020). In this estuary, the potential of intertidal sediments carrying out NO_3^- elimination was shown to be highly related to the presence of MPB (Laverman et al. 2021). However, the extent of the mudflats in the downstream Seine estuary has been reduced by a factor of 3 since 1975 and by a factor of 5 since 1875 which limits the surface colonized by MPB and their potential ecological role.

Sediment and MPB were sampled in April 2019 on the northern intertidal mudflat of the Seine estuarine mouth, Normandy, France (49°27’01.6’’N; 0°12’20.0’’E; WGS84). Sediment was collected during low tide by carefully manually pushing 10 Plexiglass® rings into the sediment until they were filled with the sediment surface. The rings have an inner diameter of 4.2 cm, a thickness of 0.4 cm and a height of 2 cm. The rings with sediment were transported in anoxic bags and stored at 4 C until the start of the experiment. Initial sediment (IS) characterization was done on sediment from two of the rings. Sediment was homogenized and 5 mL was stored at -80 C until the determination of initial *nirS*, *nirK* and *nosZ* gene copy numbers. The remaining sediment was freeze-dried (24 h) and part was conserved for further quantification of photopigment and EPS contents. The other part of the freeze-dried sediment was ground and conserved for further elemental and isotopic analyzes. MPB (*i.e.* the top 2 mm of the colonized sediment) was collected on the same site and freeze dried (24 h) before its utilization in the flow through reactor (FTR) experiment. Thereby, the added form of MPB thus corresponds to a MPB/sediment mix originating from the top 2 mm of the sediment surface covered with a natural assemblage of MPB.

2.2. Flow through reactor experiment

The 8-remaining sediment rings were used to perform a FTR experiment to evaluate the potential rates of NO_3^- reduction. Four distinct conditions including the control were performed in duplicate per condition resulting in 8 reactors. Sediment from each ring was removed, weighed, and

homogenized, then MBP were added in the form of freeze-dried powder directly to the sediment. MPB additions corresponded to control (no addition), 1, 5, and 10 % total sediment weight (hereafter named M0, M1, M5, and M10). These values were chosen in order to reach higher but realistic amounts of chl *a* observed in sediments of intertidal mudflats (Underwood and Kromkamp 1999). After being amended with MPB and carefully homogenized, a sample of each replicated condition was kept and freeze-dried (24 h) for initial characterization, while the remaining amended sediment was redistributed inside each plexiglass ring. Two filters, a 0.2 µm pore size PVDF (Durapore®) membrane filter and a glass fiber backing filter (1.2 mm thick, 4.7 cm diameter, PALL Corp., NY), were placed over the sediment surfaces at both ends of the Plexiglas® rings. The resulting sediment reactor cell was then enclosed by POM (poly-oxy methylene) Delrin® caps with in and outflow channels. A detailed description of the FTR design and the determination of potential rates can be found in Laverman et al. (2006, 2012). To ensure NO_3^- availability throughout the experiment, each ring was supplied by an inflow solution of 10mM potassium nitrate (KNO_3^-). Inflow solutions corresponded to artificial sea water where salinity was adjusted at 30 with NaCl to match the salinity measured in water from the sampling site. In addition, the inflow pH was adjusted to match the ambient conditions (pH = 8) using $NaHCO_3$ (0.2 g L^{-1}). As the process targeted in this study is anoxic (denitrification), all the input solutions were kept anoxic by purging them with O_2–free N_2 for at least 5 minutes before the start of the experiment. Moreover, the experiment was performed in dark conditions to limit the photosynthetic activity and avoid inhibitory effects or competition between diatoms and bacteria which would have influenced NO_3^- reduction rates (Bartoli et al. 2021). The experiments were run at constant temperature (21 ± 2 C) for a two-week period after a 16-hour settle time in experimental conditions. The two-week period was chosen based on previous work indicating sufficient time for the microbial community to change upon the imposed variables (Bååth et al. 1988; Laverman et al. 2015).

For 357 hours (15 days), the reactor cells were supplied with input solutions at a constant flow rate ($Q = 2 \pm 0.15$ mL h^{-1}) using a peristaltic pump (Gilson minipuls). The sediment inside the reactors was thus saturated with a saline anoxic NO_3^- solution during the entire duration of the FTR experiment. The reactor outflow samples were collected in centrifugation tubes at 4-hour intervals during the day (9am-1pm, 1pm-5pm) resulting in 2 sample collections per experimental day. The night outflow solutions (5pm-9am) were discarded. Each collected sample was conserved at 4 C and analyzed for ammonium (NH_4^+), nitrite (NO_2^-), and nitrate (NO_3^-) concentrations using a Gallery™ Discrete Analyzer (ThermoFisher scientific, Waltham, Massachusetts, USA).

The rates of reduction or production of dissolved inorganic nitrogen (DIN) in the flow-through reactors (nmol cm^{-3} h^{-1}) were calculated using the equation $R = (\Delta C \times Q)/V$ where Q is the volumetric flow rate, V the reactor volume (27.7 cm^3) and ΔC the difference in concentration of the solute between the outflow and inflow solutions. Net NO_3^- reduction rates were calculated by substituting the measured difference in NO_3^- concentration between inflow and outflow (ΔC). As NH_4^+ or NO_2^- were not supplied

throughout the inflow solutions, net NH_4^+ and NO_2^- release rates were directly determined using the outflow concentrations instead of ΔC.

At the end of the FTR experiment, the sediment from each reactor was homogenized and used for final characterization. As described for the initial sediment samples and initial MPB amended sediment, 5 mL of sediment was kept at -80 C for estimation of the densities of the denitrifying communities. The remaining sediment was freeze-dried and a part was kept for quantification of photopigment and EPS contents. The remaining freeze-dried sediment was ground and used to perform elemental and isotopic analyzes.

2.3. Characterization of denitrifying communities.

DNA was extracted from sediment (from 3 to 4.5 g wet) with the NucleoBond® RNA Soil kit and its DNA co-elution set (Macherey Nagel) according to the manufacturer's instructions and subsequently quantified and checked for purity by 260/280 (around 1.8) and 260/230 (around 2) ratio analysis with a NanoDrop 1000 Spectrophotometer (Thermo Fisher scientific). Genes encoding for enzymes implied in the denitrification process were enumerated via quantitative PCR following recommendations of Bustin et al. (2009). The following primer pairs were used: three pairs for NO_2^- reductase genes, one for *nirS* gene (nirSC1F, ATCGTCAACGTCAARGARACVGG, nirSC1R, TTCGGGTGCGTCTTSABGAAS AG, (Wei et al. 2015)) and two for *nirK* gene (cluster I, NirKC1F, ATGGCGCCATCATGGTNYTNCC, NirKC1R, TCGAAGGCCTCGATNARRTTRTG and cluster II, NirKC2F, TGCACATCGCCAACG GNATGTWYGG, NirKC2R, GGCGCGGAAGATGSHRTGRTCNACA, (Wei et al. 2015)). Two nitrous oxide reductase *nosZ* genes were used (clade I: nosZ1840F(2F), CGCRACGGCAASAAGGTSMSSGT and nosZ2090R(2R), CAKRTGCAKSGCRTGGCAGAA, (Philippot et al. 2013), clade II: 1153_nosZ8F, CTIGGICCIYTKCAYAC and 1888_nosZ29R, GCIGAICARAAITCBGTRC, (Jones et al. 2013)). Several clades or clusters were targeted in order to be the most exhaustive. PCR reactions were performed using the SensiFAST SYBR NO-ROX mix (Meridian Bioscience) in six replicates using a Wafergen SmartChip Real-time PCR system (Takara) for *nirS* and *nirK* genes and in three replicates using a LightCycler® 480 (Roche) for *nosZ* genes. DNA template quantities were normalized by dilution to reach 30 ng μL^{-1}. Negative controls, using ultra-pure water instead of templates, were performed in order to check if there was no contamination; positive controls, corresponding to plasmids containing a cloned gene of interest, allowed to determine copy numbers. Cycle number at which the fluorescence reaches a threshold (Ct) was determined with the second derivative maximum analysis method. Amplification efficiencies were determined using a calibration curve (gene copy number versus the Ct value) of positive controls by performing qPCR of 10-fold dilutions of them; absolute quantification (as gene copy number from a Ct) was recovered using the same calibration curve. The quantification limit was defined as fluorescent signals with at least 5 Ct below the signal of the negative controls.

2.4. Photopigments and EPS content

Chlorophyll *a* (chl *a*) and phaeopigment content in MPB and sediment samples were determined according to Lorenzen (1967). The pigments were extracted from 0.5 g of sediment suspended in 10 mL acetone (90%) for 12 hours in the dark at 4 C. After centrifugation (4 C, 3000 rpm, 5 min), fluorescence of the supernatant was measured using a Uvikon XL© spectrophotometer (Secomam, Aqualabo, France) before and after acidification (10 µL HCl 0.3 M per milliliter of sample).

EPS were extracted from 0.5 g of dried sediment in 15 mL centrifugation tubes with 5 mL of distilled water (MilliQ). After 1 hour of incubation at 35 C under continuous mixing (30 rpm), tubes were centrifuged (4 C, 3000 rpm, 10 min). Supernatants containing the EPS were collected in a new centrifugation tube. Low and high molecular weight EPS (LMW and HMW) were separated by incubation in ethanol (80% final concentration) for 16 hours at -20 C. HMW EPS were precipitated by cold ethanol and after centrifugation (4 C, 3000 rpm, 30 min), the supernatant which contain LMW EPS, was collected in a new tube while HMW EPS remained in the pellet. Supernatants and pellets were then dried at 50 C. The dried samples were resuspended in 1.16 mL distilled water for carbohydrate and protein quantification (1 mL and 160 µL respectively). Total carbohydrate content was determined using the phenol–sulfuric acid assay with glucose as a standard (Dubois et al. 1956) and protein content was determined using the Bradford assay reagent (Bio-Rad) with bovine serum albumin (BSA) from Sigma-Aldrich as standard (Bradford 1976). For carbohydrates, absorbance was read, after 40 minutes of incubation, using a Uvikon XL© spectrophotometer (Secomam, Aqualabo, France) at 485 nm. For proteins, absorbance was read, after 5 minutes of incubation, using a microplate reader SAFAS Xenius XL© (SAFAS Monaco) at 590 nm. All results are expressed in µg per gram of dry sediment weight (µg $gDSW^{-1}$).

2.5. Elemental and isotopic analyzes

A sub-sample of freeze-dried and crushed sediment from each replicated condition was placed into a tin capsule and used to determine the N_{tot}. Another sub-sample was acid-treated with 2N HCl to remove the carbonate and was subsequently rinsed with deionized water. The carbonate-free sub-sample was dried at 60 C, and manually ground before being placed into a tin capsule for the determination of C_{org} and $\delta^{13}C$. Contents and isotopic compositions of total organic carbon and total nitrogen (C_{org}; N_{tot}; $\delta^{13}C$) were determined by Elemental Analysis –Isotope Ratio Mass Spectrometry (EA-IRMS) Vario pyro cube (Micromass Isoprime). The standard gas was calibrated in relation to the international standard (PeeDee Belemnite-190PDB). N_{tot} and C_{org} were expressed as percentage of the dry sediment mass and the C_{org}/N (molar:molar) was calculated.

2.6. Statistical analysis

For each tested condition (M0, M1, M5, and M10), the potential significant variability of measured rates throughout the duration of the experiment was tested by one-way repeated measures

analysis of variance (RM-aov) using Sigma-Plot 12 software. Shapiro-Wilk normality tests and Bartlett equal variance tests were used, and in the non-parametric cases, RM-aov on ranks were performed. Both RM-aov were followed by a Tukey-test in order to discriminate differences. In addition, to discriminate significant differences between the tested conditions throughout the experiment, Split-plot ANOVA (Split-plot aov) were performed on R software (version 4.0.2).

In order to distinguish the effect of the MPB addition on nitrogen transformation, considering an adaptation period of two weeks for the microbial community, the rates during the last day of the incubations (2 samples per replicate resulting in 4 values) were compared to the other parameters measured at the end of the experiment (chl *a*, C:N ratio, $\delta^{13}C$, gene copy numbers). After testing the normality and equal variance tests as previously mentioned, a one-way analysis of variance (aov) followed by a Tukey-test were performed; a Kruskal-Wallis test followed by a Dunn test were performed if application conditions were not met.

A principal component analysis was performed using the package "FactoMineR" in R on the data frame represented by the differences measured between the initial and the final values measured. Correlation tests were then realized to interpret the PCA plot.

3. Results

3.1. Sediment characteristics

Sediment used in this experiment had mean silt (particles < 63 µm) and water content of 25.6 % and 40.5 %, respectively. The addition of freeze-dried MPB induced an increase in nitrogen and carbon contents in sediment (table 1) resulting in an increasing C/N ratio from 10.3 to 10.9. The MPB addition also led to an increase of labile carbon, as illustrated by the increase of EPS contents, and in an increase of the chl *a* content of 42%, 202%, and 402% respectively in M1, M5, and M10 compared to M0. The $\delta^{13}C$ showed higher values for M5 and M10 (on average -24.4 ± 0.4) than for M0 and M1 (on average -25.5 ± 0.4).

After the 357 hours incubation of the different reactors under anoxic conditions and with continuous supply of NO_3^-, the different organic carbon contents (total C_{org}, Chl *a*, EPS) in sediments showed lower values in comparison to values before incubation (table 1). The greatest difference in sediment characteristics before and after the experiment was observed for LMW carbohydrate EPS (table 1), which decreased by 61 -71% over the course of the incubations. Similarly, HMW carbohydrate EPS and HMW proteins also decreased by 14-41% and 22-64%, respectively. In contrast, the LMW proteins increased over the course of the incubation by 7-30%. The chl *a* content also decreased by 4-38% while the phaeopigment content increased by 13-178%. Nitrogen and carbon contents decreased by 16-25% and 18-27% respectively leading to low variation of the C:N ratios up to 7%. The $\delta^{13}C$ only decreased by 0.4-1.3%.

3.2. Nitrate reduction and nitrite release rates

The constant supply of NO_3^- to the sediment in the control condition (M0) resulted in net NO_3^- reduction rates with an average of 150 ± 3 nmol NO_3^- cm^{-3} h^{-1} during the first 24 hours of experiment. These rates then decreased significantly (RM-aov; p-value < 0.001) over the duration of the 357 hours of incubation (fig. 1-A) down to 19 ± 6 nmol NO_3^- cm^{-3} h^{-1} the last day of experiment (fig. 2-A). In parallel, the net NO_2^- release rate increased over the first 100 hours to a maximum value of 35 ± 4 nmol NO_2^- cm^{-3} h^{-1} (fig. 1-B). After that, the NO_2^- release rates decreased to an average of 14 ± 3 nmol NO_2^- cm^{-3} h^{-1} the last day of experiment (fig. 2-B).

The same NO_3^- supply with addition of MPB to the sediment resulted in significantly higher net NO_3^- reduction rates for each condition correlating positively with the amount of MPB added (Split-plot aov; p-values < 0.001). In comparison to the control M0, the net NO_3^- reduction rates significantly increased (RM-aov; p-values < 0.001) over the first 100 hours of incubation to a maximum of 276, 383, and 400 nmol NO_3^- cm^{-3} h^{-1} respectively for M1, M5, and M10 (fig. 1-A). These rates corresponded respectively to an increase of 85%; 156% and 267% compared to M0. Then, net NO_3^- reduction rates significantly decreased (RM-aov; p-values < 0.001) down to 71 ± 10, 97 ± 1, and 140 ± 26 nmol NO_3^- cm^{-3} h^{-1} at the end of the experiment respectively for M1, M5, and M10, but remaining significantly higher than M0 (aov; p-value < 0.001; fig. 2-A). The NO_2^- release rates were also significantly higher in amended conditions than in M0 (Split-plot aov; p-values < 0.001) over the 100 first hours of incubation reaching maximal values of 124 ± 11, 119 ± 20, and 148 ± 17 nmol NO_2^- cm^{-3} h^{-1} respectively for M1, M5 and M10 (Fig. 1-B). During the rest of the experiment, NO_2^- release rates decreased and no significant differences were recorded the last day of the experiment (Kruskal-Wallis; p-values = 0.44, 0.07, and 0.45 respectively for M1, M5, and M10) with values of 15 ± 3, 14 ± 4, and 32 ± 5 nmol NO_2^- cm^{-3} h^{-1} respectively for M1, M5, and M10 (fig. 2-B).

3.3. Estimation of carbon consumption for denitrification

By considering the C_{org} originated from the added MPB (C_{org} content of 4%), it was estimated that its addition has led to an increase of 22, 108, and 216 mg of C_{org} from MPB origin (respectively in M0, M1, M5, M10). With an average NO_3^- reduction rate of 73 nmol cm^{-3} h^{-1}, it was estimated that a total of approximatively 10 mg N-NO_3^- was reduced in the non-amended control reactor (27.7 cm^3), over the duration of the experiment (357 hours). In the same way, approximatively 17, 28, and 44 mg of N-NO_3 were reduced respectively for M1, M5, and M10. Knowing that 5 moles of carbon are used during the complete denitrification process when 4 moles of nitrogen are reduced to nitrogen gas ($4NO_3^- + 5CH_2O + 4H^+ \rightarrow 5CO_2 + 2N_2 + 7\ H_2O$), and assuming that denitrification was the only N-reducing process, on average 11, 18, 30, and 47 mg of carbon were respectively used for denitrification in M0, M1, M5, and M10.

Considering the total amount of carbon consumed during the two-week experiment (table 1; 510, 380, 590, and 490 mg), it can be thus be estimated that approximately 2.1, 4.7, 5.1, and 9.7% of the organic carbon degraded during the two-weeks incubation could have been used for denitrification

(respectively in M0, M1, M5, M10). In addition to this, as it was the added MPB carbon that drove the increase in net NO_3^- reduction rates, it is hypothesized that the majority of the added MPB was used in M1 (82%) and approximatively 28 and 22% in M5 and M10.

Knowing that the proportion of carbon in glucose represents 46.7% of the molecular weight and that carbohydrate EPS were expressed in glucose equivalents, it was estimated that LMW carbohydrate EPS represented between 0.77 to 1.14% of the total carbon consumed while HMW carbohydrates EPS represented between 0.27 and 0.35% for the different conditions (M0 to M10). By considering that all consumed EPS were used for denitrification, it was roughly estimated that LMW carbohydrates represented 36, 24, 17, and 12% of the carbon consumed for denitrification (18, 30, and 47 mg of carbon previously estimated) and 14, 8, 2, and 3% for HMW carbohydrates.

3.4. Ammonium release rate

The control sediment (M0) showed a mean net NH_4^+ release rate of 7 ± 4 nmol NH_4^+ cm^{-3} h^{-1} with no significant variability (RM-aov; p-value = 0.52) along the duration of the experiment (fig. 3). In MPB amended sediments, significantly higher net NH_4^+ release rates were recorded for each condition (Split-plot aov; p-value < 0.05 for M1 and p-values < 0.001 for M5 and M10), positively correlated to the amount of MPB added (fig. 3). More specifically, after addition of MPB, a significant increase of net NH_4^+ release rates (RM-aov; p-values < 0.05) was recorded over the first 100 hours of incubation up to a maximum of 18 ± 1, 73 ± 2, and 127 ± 14 nmol NH_4^+ cm^{-3} h^{-1} respectively for M1, M5, and M10. After that, net NH_4^+ release rates decreased over the duration of the experiment. The last day of the experiment, the net NH_4^+ release rates were not significantly different for M0, M1, and M5 (Kruskal-Wallis; p-values = 0.48 and 0.13 respectively for M1 and M5) which presented on average values of 1.6 ± 0.5, 1.7 ± 0.7 and 8.7 ± 1.2 nmol NH_4^+ cm^{-3} h^{-1} respectively (fig. 4). In contrast, M10 showed a significant higher net NH_4^+ release rates (Kruskal-Wallis; p-value < 0.05) with 13.9 ± 2.6 nmol NH_4^+ cm^{-3} h^{-1} (fig. 4).

3.5. Microbial denitrifying communities

Approximately 3x more DNA was extracted from sediments at the end of the two week incubation (between 13.8 and 19.3 µgDNA $gDSW^{-1}$; table 2) than at the beginning (4.3 µgDNA $gDSW^{-1}$). Using quantitative PCR (qPCR) to measure the gene abundance, the initial sediment sample showed on average $6.3\times10^7 \pm 1.7\times10^7$ copies of *nir* gene $gDSW^{-1}$ and on average $3.7\times10^9 \pm 0.6\times10^9$ copies of *nosZ* gene $gDSW^{-1}$. Compared to the initial sediment, after the 357 hours of incubation, the numbers of *nir* increased two orders of magnitude (from 10^7 to 10^9) and one order of magnitude for *nosZ* gene copy numbers (table 2). With the MPB addition, the increase of *nir* genes (fig. 5-A) was even higher with an increase of 52%, 101%, and 160% compared to M0 respectively for M1, M5, and M10. For the *nosZ* genes (fig. 5-B), no difference was observed between treatments. Both functional genes exhibited a change in gene contribution over the course of the incubation: for *nir* genes, the *nirS* contribution

increased in default of *nirK* while for *nosZ* genes, clade I *nosZ* increased in default to clade II *nosZ* (table 2; fig. 5).

3.6. Relationship between variables during the incubation experiment

A principal component analysis (PCA) was performed on the values representing the differences between the parameters before and after experimentation for sediment characteristics (table 2; C, N, Chl a, and EPS consumed besides phaeopigment and protein LMW EPS produced. In addition, the amount of NO_3^- reduced (NR) and the quantities of NH_4^+ and NO_2^- released (AR and NiR) during the experimental time were added as well as the difference in the abundance of denitrification-related genes (*nirK*, *nirS*, clade I *nosZ*, and clade II *nosZ*).

The first and second dimension of the PCA explained 83.7% of the total inertia (fig. 6). The first dimension, with 57.06% of the variance showed the highest contributions for the LMW carbohydrates consumption, NO_3^- reduction, NH_4^+ and NO_2^- release and the denitrifying gene abundances. In detail, the LMW carbohydrates accounted for 11.6%, NO_3^- reduced for 11.6%, NH_4^+ and NO_2^- released respectively for 11.2% and 9% while the microbial denitrifying communities accounted for 8.5%, 11.7%, 6.4%, and 9.7% respectively for *nirK*, *nirS*, clade I *nosZ*, and clade II *nosZ*. The second dimension (26.65% of variance) showed the highest contributions for the sedimentary nitrogen and carbon consumed (19.1% and 14.2% respectively), the quantity of HMW EPS (19.2% and 15.8% respectively for carbohydrates and proteins), chlorophyll *a* consumed (15%). The third dimension (16.3% of variance) showed the highest contribution for the phaeopigments released (33.5%).

The correlation tests allowed interpretation of the PCA plot showing significant positive correlations between the number of *nirS* gene copies number and both the NO_3^- reduced (Pearson corr. coef. = 0.99; p-value < 0.01; R^2 = 0.99) and the NH_4^{+-} released (Pearson corr. coef. = 0.97; p-value < 0.05; R^2 = 0.95). In contrast, the *nirS* gene copies number showed a negative correlation with the LMW carbohydrates (Pearson corr. coef. = - 0.99; p-value < 0.01; R^2 = 0.99). As a consequence, the LMW carbohydrates showed negative correlations with both the NO_3^- reduced (Pearson corr. coef. = -0.98; p-value < 0.05; R^2 = 0.97) and the NH_4^+ released (Pearson corr. coef. = -0.96; p-value < 0.05; R^2 = 0.92) while a positive correlation was recorded between the NO_3^- reduced and the NH_4^+ released (Pearson corr. coef. = 0.99; p-value < 0.05; R^2 = 0.98). A negative correlation was also observed between the clade II *nosZ* gene copies number and the NO_2^- released (Pearson corr. coef. = -0.95; p-value = 0.05; R^2 = 0.90). The other Pearson correlations tested between variables were not significant (p-values > 0.05).

4. Discussion

Our results confirm by using a controlled flow through reactor (FTR) experiment that NO_3^- reduction in intertidal sediments is limited by labile carbon availability, and highlight the important contribution of the microphytobenthos (MPB) on NO_3^- reduction rates and on the denitrifying microbial communities.

The chlorophyll *a* concentrations obtained upon addition of MPB in this study (between 8 and 29 µg chl *a* $gDSW^{-1}$) were higher than the biomass usually recorded on the sampled mudflat ranging from 0.2 to 11.2 µg chl *a* gDW^{-1} (Morelle et al. 2020). Nevertheless, these values were lower than the range of MPB biomass measured up to 80 µg chl *a* $gDSW^{-1}$ in some other European and American estuarine systems (Underwood and Kromkamp 1999). As in a majority of estuarine systems, NO_3^- concentrations are elevated (between 0.5 and 7 mg L^{-1}) in the Seine estuarine waters (Morelle et al. 2018). Thereby, our results suggest that the microbial activity is especially limited by the availability of the labile carbon (MPB) in associated mudflats than by NO_3^- availability. Indeed, the highest addition of MPB led to a maximal NO_3^- reduction rate of 5.6 mgN-NO_3^- L^{-1} h^{-1} (400 nmol NO_3^- cm^{-3} h^{-1}). Moreover, by confirming that bacteria preferentially use decomposing MPB and labile extracellular polymeric substances as a carbon substrate for NO_3^- reduction, our results confirm that the diminution of natural mudflat surface which entail decline of the microphytobenthos growth (Lesourd et al. 2016; Morelle et al. 2020) must have drastically reduce the potential NO_3^- removal capacities in estuaries.

4.1. Microphytobenthos stimulates nitrate reduction

The increase in $\delta^{13}C$ observed in M5 and M10 confirmed the addition of MPB in sediment which is known to present a higher $\delta^{13}C$ than intertidal sediment (Lee et al. 2021). The highest addition of MPB performed in this study (10% total sediment weight) led to a threefold increase of NO_3^- reduction rates (up to 267%) compared to the control condition. With MPB addition corresponding to 1% and 5% of the total sediment weight, the net NO_3^- reduction rates showed an increase of 85% and 156%. These increases highlight the important contribution of the MPB to NO_3^- reduction which could even represent between 22% (M10) and 82% (M1) if denitrification is considered as the only NO_3^- reduction process and responsible for the carbon degradation. As the increase in net NO_3^- reduction rates were observed during the first 100 hours of the experiment before net NO_3^- reduction rates decreased, it confirms the rapidly and labile nature of the major compounds of the MPB. MPB biomass represents indeed a labile carbon source, without recalcitrant compounds like cellulose and lignin (Kawaida et al. 2019). MPB contributes to sediment organic matter through carbohydrates, proteins, phospholipid linked fatty acids, hydrolysable amino acids, or pigments including chlorophyll (Hardison et al. 2013).

The EPS present in MPB add a significant value for heterotrophic processes since they contain labile organic carbon (Van Duyl et al. 1999; Welker et al. 2002; Tobias et al. 2003). Indeed, in addition to an overall decrease in organic carbon with MPB addition, we observed a decrease in both carbohydrate and protein EPS (on average 68% and 28% for LMW and HMW carbohydrates and approximatively 46% of the HMW proteins). Previous studies suggested that the LMW fraction is the most labile and immediately used by bacteria rather than HMW polymers which require more energy in producing exoenzymes for hydrolytic activity (Sundh 1992; Welker et al. 2002). This could explain the higher decrease of LMW rather than HMW carbohydrates. Moreover, the quantities of LMW carbohydrates consumed were significantly higher in amended sediments while the decrease in amount

of HMW carbohydrates showed no significant differences with the control. These results combined with the increase in NO_3^- reduction rates suggest that EPS, and especially LMW carbohydrates, are being used as a carbon substrate for NO_3^- reduction in this experiment. If considering denitrification as the only NO_3^- reduction process, our result even suggest that carbohydrates EPS could contributed between 14 and 50% to the carbon consumption for denitrification. It is more complicated to estimate the contribution of protein EPS, but this fraction of EPS often represents a minor part of the total EPS content (Morelle et al. 2020) and thus must represent a smaller part of the consumed carbon. Especially since in our experiment the LMW proteins EPS increased by about 22%.This could be the result of the degradation of HMW proteins since LMW compounds are considered as the hydrolytic results of HMW EPS breakdown (Orvain et al. 2014). The protein production could also be related to the development of the microbial biomass which could also have secreted EPS and especially proteins to form a biofilm matrix (Gerbersdorf and Wieprecht 2015). Overall, it seems that carbohydrates were more easily used than protein EPS which is in agreement with previous results that consider carbohydrates as the most readily available organic fraction and labile compounds from MPB (Welker et al. 2002). Nevertheless, our results show that a large amount of carbon disappears without NO_3^- being used as an electron acceptor since the amount of carbon used is higher than the amount required for the performed NO_3^- reduction. Part of this can be explained by the use of carbon with other electron acceptors present in the sediment (iron oxides) or fermentation (Abell et al. 2009), whereas another part of the organic carbon may have leached from the sediment.

Our results also suggest that other degraded MPB cell components contribute to the carbon budget of these sediments. As NO_3^- reduction rates increased, chl *a* content decreased and phaeopigment content increased. The increase in phaeopigments, the degraded form of chl *a*, suggests an increase of the algal biomass degradation which can then be used as carbon source for NO_3^- reduction. This agrees with a previous study, showing a stimulation of denitrification rates by the addition of senescing algal biomass providing N and labile C to denitrifiers in agricultural headwater stream sediments (McMillan et al. 2010). However, the MPB added was a natural biofilm that may have contained other sources of carbon not from microalgae origin which could have been used as carbon source for degradation. The increased NH_4^+ release in the higher MPB treatments (M5 and M10) suggests that more organic matter was decomposed in these treatments, as NH_4^+ is a primary product of organic matter decomposition (Lemley et al. 2014). The higher net NO_3^- reduction rates measured in M1 compared to M0, whereas the net NH_4^+ release rates were similar, suggests the use of organic carbon releasing less NH_4^+ such as glucose or other organic compounds lacking an amino ($-NH_3^+$) group thus resulting in relative low ammonification. Overall, these results confirm experimentally the assumption that microbes use both decomposing MPB (Nielsen et al. 2004) and labile EPS as a carbon substrate for NO_3^- reduction (Tobias et al. 2003; Hope et al. 2020).

In parallel to denitrification, part of the NO_2^- produced upon NO_3^- reduction could have been partly reduced to NH_4^+ via DNRA or used through the annamox process. DNRA conserves nitrogen in

473 the ecosystem as NH_4^+, therefore not resulting in the production of N_2O. The net NH_4^+:NO_3^-rates ratio
474 illustrates either the transformation of NO_3^- into NH_4^+ or the NH_4^+ released after degradation of organic
475 matter. After the 2-week incubation, the percentage of NH_4^+ produced per NO_3^- reduced increased with
476 the proportion of MPB added (2%, 9% and 10% respectively for M1, M5, and M10) but was comparable
477 to M0 (9%). The reduction of NO_3^-, via DNRA would lead to an elevated ratio of NH_4^+ produced per
478 NO_3^- reduced. A rough estimate shows that considering a C/N ratio ranging between 9 and 12 for the
479 organic matter and added biomass, an organic carbon molecule oxidized would release between 0.08
480 and 0.11 molecules of NH_4^+. Per molecule NO_3^- reduced to N_2, 1.25 molecules of carbon are oxidized
481 resulting in 0.1 to 0.14 NH_4^+ molecules produced per NO_3^- reduced or a ratio of 10 to 14%. This is in
482 good agreement with the net NH_4^+:NO_3^-rates ratios (between 9 to 10%) determined, indicating that
483 DNRA is unlikely to play an important role in these benthic sediments. The anammox process could
484 also have partly used the NH_4^+ and NO_2^- released and have produced N_2 but this study does not allow us
485 to quantify this process.
486
487 **4.2. The impact of microphytobenthos on microbial abundance and denitrification efficiency.**
488 Our results confirm that microbes use an important part of the available carbon from MPB
489 (Soares and Rousk 2019) which is reinforced by the correlations observed at the end of the experiment
490 between the copy numbers of *nirS* gene and both the LMW carbohydrates EPS and the NO_3^- reduced.
491 The increase in microbial DNA extracted between the initial sediment and sediments incubated for 2
492 weeks under NO_3^- reducing conditions, including the non MPB-amended control, prove increase of the
493 microbial biomass by means of DNA quantification (Semenov et al. 2018). Moreover, the significant
494 increase in microbial activity as net NO_3^- reduction rates upon the addition of NO_3^- and MPB, with a
495 strong impact of the amount of added MPB as shown in Figure 2A, confirms the growth of NO_3^-
496 reducers. This was also reflected by the increase in the number of functional gene copies for *nirK/nirS*
497 and *nosZ* which indicates active growth of denitrifying microbes in these estuarine sediments (Smith et
498 al. 2007).
499 Whereas the NO_2^- reductase gene copy numbers (*nir*) show a significant increase with the MPB
500 additions, the total nitrous oxide reductase (*nosZ*) gene copy numbers remain unchanged (Table 2,
501 Figure 5). Interestingly, the increase in NO_2^- reductase gene copy numbers is mainly due to an increase
502 in *nirS* gene copies, whereas *nirK* gene copies significantly decreased. The denitrifiers possessing *nirS*
503 genes developed and grew faster than those possessing *nirK* genes upon the addition of the MPB
504 biomass. This shows that the imposed conditions (anoxic, NO_3^- supply) and the increasing amounts of
505 organic carbon in the form of MPB favored the growth of organisms harboring *nirS* gene. A more
506 important abundance of *nirS* gene correlated to high NO_3^- load was already observed by Lee and Francis
507 (2017) in different sediments of the San Francisco Bay. This result of the current study corroborates that
508 these variables (anoxia, NO_3^- supply, MPB) play a significant role in the capacity of the sediment to
509 reduce NO_3^- via denitrification (Papaspyrou et al. 2014). It has been suggested that bacteria possessing

510 *nirS* genes are generally complete denitrifiers rather than *nirK* containing organisms (Graf et al. 2014);
511 this might indicate that the bacterial growth upon MPB biomass stimulated those capable of full
512 denitrification. This would be in line with the slight increase in gene copy number of clade I *nosZ* which
513 are more likely to be complete denitrifiers, as 83% of genomes with clade I *nosZ* also possess *nir* genes
514 (Graf et al. 2014; Hallin et al. 2018). In comparison, microbes harboring clade II *nosZ* genes are also
515 called "non-denitrifier" nitrous oxide reducers as these microbes often lack NO_3^- and NO_2- reductase
516 genes (Bertagnolli et al. 2020). The stimulation of organisms carrying out full denitrification during the
517 incubation period and related to the addition of organic carbon would require a metagenomics analysis,
518 allowing reconstruction of genomes and confirmation of an increase of 'complete denitrifiers'.
519 Compared to the initial sediment, *nir* copy numbers at the end of the incubation increased two
520 orders of magnitude (from 10^7 to 10^9) and one order of magnitude for *nosZ* copy numbers at the end of
521 the incubation. However, gene copy numbers of *nosZ* exceeded those of *nirS* and *nirK* in both the initial
522 and incubated sediment. Whether the difference in gene copy numbers of the different reductases can
523 be translated in different activities is unclear. The increase of NO_2^- reductases upon the production of
524 NO_2^- appears efficient as little NO_2^- accumulated. The subsequent production and reduction of nitrous
525 oxide gas was not determined but the high abundance of *nosZ* gene copy numbers (compared to *nir* gene
526 copy numbers) leads to believe that they were initially sufficient to ensure the reduction of nitrous oxide.
527 The total number of *nir* genes (*nirK* and *nirS*) showing increasing values in relation with the
528 amount of added MPB (fig. 5) highlights that presence of organic carbon from microphytobenthic origin
529 positively influenced the growth of NO_2^- reducers and their potential reduction to NO. Considering that
530 the amount of NO_2^- produced is a trigger for NO_2^- reductases, the increase of NO_3^- reduction rates (or
531 total NO_2^- release rates) is in good agreement with the increase of the total number of *nir* gene copy
532 numbers. This is reinforced by the net NO_2^- release rates which remain low along the experiment
533 (< 100 nmol NO_2^- cm^{-3} h^{-1}), implying that most of the NO_3^- reduced to NO_2^- is reduced further.
534 Difference between the total and net NO_2^- release rates suggests that 66 – 72 % of the NO_2^- was further
535 reduced to NO (N_2O and N_2) or other (e.g. NH_4^+). This calculation considers the initial accumulation of
536 NO_2^- which is a common phenomenon usually explained via the induction of NO_2^- reduction genes upon
537 an increase in NO_2^- (Betlach and Tiedje 1981). At the end of the two-week incubation, the proportion of
538 NO_3^- reduced to NO_2^- (estimated by the net NO_2^-:NO_3^- rates ratio), and thus not further reduced to N_2 or
539 NH_4^+, was higher in the non-amended sediment (on average 80 %). This ratio was lower when MPB
540 was added, between 14 to 23% for the different additions, indicating a higher reduction of NO_2^- into N_2
541 or NH_4^+. This is also in good agreement with the increasing numbers of *nirS* gene copy numbers and a
542 slight increase of the clade I *nosZ* genes indicating a significant role and increase of denitrification upon
543 the addition of MPB biomass as carbon source.
544
545 **5. Conclusion**

This study experimentally demonstrated, in Seine estuary sediments, that microphytobenthos plays a crucial role in benthic nitrogen fluxes via nitrate reduction and especially denitrification. This crucial role being made through the use, by denitrifiers, of the labile extracellular polymeric substances secreted by the MPB which might contribute up to 50% of the carbon used for denitrification. But also, through the use of decomposing microphytobenthic components. In addition, the results showed that addition of microphytobenthos led to a significant shift in the denitrifier community composition favoring complete denitrifiers and the complete reduction of NO_3^- into N_2 leading to efficient nitrogen removal from waters. Beyond the role played by intertidal mudflats and microphytobenthos on nitrogen cycling, the potential role of adjacent intertidal salt marshes to carry out NO_3^- elimination processes was also highlighted in this estuary (Laverman et al. 2021). These results are thus all the more important in the context of climate change since the increase in extreme climatic events and sea level rise represent a serious threat to the presence of many estuarine intertidal mudflats, adjacent salt marshes and their associated ecological values.

Acknowledgments

This work was financed by the GIP Seine-Aval project PHARESEE (Program SA6). The authors acknowledge Francis Orvain and Arnaud Huguet (PIs of the project), Romain Chocun-Collet and Etienne Laborde for their participation in the experimentation. The ECOCHIM platform of Rennes University is acknowledged for help with the Gallery device; the Molecular Ecology Platform $(PEM)^2$ for the DNA extractions and qPCRs. The authors also acknowledge Romain Causse-Vedrines from the Biogenouest Genomics and Ecological Genomics (EcogenO) core facility of Rennes (Biosit/OSUR) for assistance with the Wafergen SmartChip Real-time PCR system. The authors also acknowledge the two anonymous reviewers that helped significantly improvement of the manuscript.

References

Abell, J., A. M. Laverman, and P. Van Cappellen. 2009. Bioavailability of organic matter in a freshwater estuarine sediment: Long-term degradation experiments with and without nitrate supply. Biogeochemistry **94**: 13–28. doi:10.1007/s10533-009-9296-x

Bååth, E., S. Olsson, and A. Tunlid. 1988. Growth of bacteria in the rhizoplane and the rhizosphere of rape seedlings. FEMS Microbiol. Lett. **53**: 355–360. doi:10.1016/0378-1097(88)90501-0

Babbin, A. R., A. Jayakumar, and B. B. Ward. 2016. Organic Matter Loading Modifies the Microbial Community Responsible for Nitrogen Loss in Estuarine Sediments. Microb. Ecol. **71**: 555–565. doi:10.1007/s00248-015-0693-5

Barbier, E., S. Hacker, C. Kennedy, E. Koch, A. Stier, and B. Silliman. 2011. The value of estuarine and coastal ecosystem services. Ecol. Monogr. **81(2)**: 169–193.

Bartoli, M., D. Nizzoli, M. Zilius, and others. 2021. Denitrification, Nitrogen Uptake, and Organic Matter Quality Undergo Different Seasonality in Sandy and Muddy Sediments of a Turbid Estuary. Front. Microbiol. **11**. doi:10.3389/fmicb.2020.612700

Bastviken, S. K., P. G. Eriksson, A. Ekström, and K. Tonderski. 2007. Seasonal denitrification potential in wetland sediments with organic matter from different plant species. Water. Air. Soil Pollut. **183**: 25–35. doi:10.1007/s11270-007-9352-x

Bellinger, B. J., G. J. C. Underwood, S. E. Ziegler, and M. R. Gretz. 2009. Significance of diatom-

588 derived polymers in carbon flow dynamics within estuarine biofilms determined through isotopic
589 enrichment. Aquat. Microb. Ecol. **55**: 169–187. doi:10.3354/ame01287
590 Bertagnolli, A. D., K. T. Konstantinidis, and F. J. Stewart. 2020. Non-denitrifier nitrous oxide reductases
591 dominate marine biomes. Environ. Microbiol. Rep. **12**: 681–692. doi:10.1111/1758-2229.12879
592 Betlach, M. R., and J. M. Tiedje. 1981. Kinetic Explanation for Accumulation of Nitrite, Nitric Oxide,
593 and Nitrous Oxide During Bacterial Denitrification †. Appl. Environ. Microbiol. **42**: 1074–1084.
594 doi:10.1128/aem.42.6.1074-1084.1981
595 Billen, G., and J. Garnier. 2007. River basin nutrient delivery to the coastal sea: Assessing its potential
596 to sustain new production of non-siliceous algae. Mar. Chem. **106**: 148–160.
597 doi:10.1016/j.marchem.2006.12.017
598 Billen, G., J. Garnier, J. Némery, M. Sebilo, A. Sferratore, S. Barles, P. Benoit, and M. Benoît. 2007. A
599 long-term view of nutrient transfers through the Seine river continuum. Sci. Total Environ. **375**:
600 80–97. doi:10.1016/j.scitotenv.2006.12.005
601 Bouillon, S., and H. T. S. Boschker. 2006. Bacterial carbon sources in coastal sediments: a review based
602 on stable isotope data of biomarkers. Biogeosciences **3**: 175–185. doi:10.5194/bgd-2-1617-2005
603 Bradford, M. M. 1976. A rapid and sensitive method for the quantitation of microgram quantities of
604 protein utilizing the principle of protein-dye binding. Anal. Biochem. **72**: 248–254.
605 De Brouwer, J. F. C., T. R. Neu, and L. J. Stal. 2006. On the function of secretion of extracellular
606 polymeric substances by benthic diatoms and their role in intertidal mudflats: A review of recent
607 insights and views, p. 45–61. *In* J.C. Kromkamp, J.F.C. De Brouwer, G.F. Blanchard, R.M. Forster,
608 and V. Créac [eds.], Functioning of microphytobenthos in estuaries. Royal Netherlands Academy
609 of Arts and Sciences.
610 Bustin, S. A., V. Benes, J. A. Garson, and others. 2009. The MIQE guidelines: Minimum information
611 for publication of quantitative real-time PCR experiments. Clin. Chem. **55**: 611–622.
612 doi:10.1373/clinchem.2008.112797
613 Costanza, R., R. Arge, R. De Groot, and others. 1997. The value of the world ' s ecosystem services and
614 natural capital. Nature **387**: 253–260. doi:10.1038/387253a0
615 Decleyre, H., K. Heylen, C. Van Colen, and A. Willems. 2015a. Dissimilatory nitrogen reduction in
616 intertidal sediments of a temperate estuary: Small scale heterogeneity and novel nitrate-to-
617 ammonium reducers. Front. Microbiol. **6**. doi:10.3389/fmicb.2015.01124
618 Decleyre, H., K. Heylen, K. Sabbe, B. Tytgat, D. Deforce, F. Van Nieuwerburgh, C. Van Colen, and A.
619 Willems. 2015b. A doubling of microphytobenthos biomass coincides with a tenfold increase in
620 denitrifier and total bacterial abundances in intertidal sediments of a temperate estuary. PLoS One
621 **10**: 1–23. doi:10.1371/journal.pone.0126583
622 Dodla, S. K., J. J. Wang, R. D. DeLaune, and R. L. Cook. 2008. Denitrification potential and its relation
623 to organic carbon quality in three coastal wetland soils. Sci. Total Environ. **407**: 471–480.
624 doi:10.1016/j.scitotenv.2008.08.022
625 Dubois, M., K. A. Gilles, J. K. Hamilton, Pa. Rebers, and F. Smith. 1956. Colorimetric method for
626 determination of sugars and related substances. Anal. Chem. **28**: 350–356.
627 Van Duyl, F. C., B. De Winder, A. J. Kop, and U. Wollenzien. 1999. Tidal coupling between
628 carbohydrate concentrations and bacterial activities in diatom-inhabited intertidal mudflats. Mar.
629 Ecol. Prog. Ser. **191**: 19–32. doi:10.3354/meps191019
630 Erisman, J. W., M. A. Sutton, J. Galloway, Z. Klimont, and W. Winiwarter. 2008. How a century of
631 ammonia synthesis changed the world. Nat. Geosci. **1**: 636–639. doi:10.1038/ngeo325
632 Eyre, B. D., J. M. Oakes, and J. J. Middelburg. 2016. Fate of microphytobenthos nitrogen in subtropical
633 subtidal sediments: A 15N pulse-chase study. Limnol. Oceanogr. **61**: 2108–2121.
634 doi:10.1002/lno.10356
635 Eyre, B. D., I. R. Santos, and D. T. Maher. 2013. Seasonal, daily and diel N2 effluxes in permeable
636 carbonate sediments. Biogeosciences **10**: 2601–2615. doi:10.5194/bg-10-2601-2013
637 Fernandes, S. O., P. Dutta, M. J. Gonsalves, P. C. Bonin, and P. A. LokaBharathi. 2016. Denitrification
638 activity in mangrove sediments varies with associated vegetation. Ecol. Eng. **95**: 671–681.
639 doi:10.1016/j.ecoleng.2016.06.102
640 Galloway, J. N., F. J. Dentener, D. G. Capone, and others. 2004. Nitrogen cycles: past, present, and
641 future. Biogeochemistry **70**: 153–226.
642 Geider, R. J., E. H. Delucia, P. G. Falkowski, and others. 2001. Primary productivity of planet earth :

biological determinants and physical constraints in terrestrial and aquatic habitats.
Gerbersdorf, S. U., and S. Wieprecht. 2015. Biostabilization of cohesive sediments: Revisiting the role of abiotic conditions, physiology and diversity of microbes, polymeric secretion, and biofilm architecture. Geobiology **13**: 68–97. doi:10.1111/gbi.12115
Van de Graaf, A. A., A. Mulder, P. De Bruijn, M. S. M. Jetten, L. A. Robertson, and J. G. Kuenen. 1995. Anaerobic oxidation of ammonium is a biologically mediated process. Appl. Environ. Microbiol. **61**: 1246–1251. doi:10.1128/aem.61.4.1246-1251.1995
Graf, D. R. H., C. M. Jones, and S. Hallin. 2014. Intergenomic comparisons highlight modularity of the denitrification pathway and underpin the importance of community structure for N2O emissions. PLoS One **9**: 1–20. doi:10.1371/journal.pone.0114118
Grizzetti, B., F. Bouraoui, G. Billen, and others. 2011. Nitrogen as a threat to European water quality, p. 379–404. *In* M.A. Sutton, C.M. Howard, J.W. Erisman, G. Billen, A. Bleeker, P. Grennfelt, V.H. Grinsven, and B. Grizzetti [eds.], European Nitrogen Assessment. Cambridge University Press, UK.
Hallin, S., L. Philippot, F. E. Löffler, R. A. Sanford, and C. M. Jones. 2018. Genomics and Ecology of Novel N2O-Reducing Microorganisms. Trends Microbiol. **26**: 43–55. doi:10.1016/j.tim.2017.07.003
Hardison, A. K., E. A. Canuel, I. C. Anderson, C. R. Tobias, B. Veuger, and M. N. Waters. 2013. Microphytobenthos and benthic macroalgae determine sediment organic matter composition in shallow photic sediments. Biogeosciences **10**: 5571–5588. doi:10.5194/bg-10-5571-2013
Hillebrand, H., J. M. Cowles, A. Lewandowska, D. B. Van de Waal, and C. Plum. 2014. Think ratio! A stoichiometric view on biodiversity-ecosystem functioning research. Basic Appl. Ecol. **15**: 465–474. doi:10.1016/j.baae.2014.06.003
Hope, J. A., D. M. Paterson, and S. F. Thrush. 2020. The role of microphytobenthos in soft-sediment ecological networks and their contribution to the delivery of multiple ecosystem services. J. Ecol. **108**: 815–830. doi:10.1111/1365-2745.13322
Hume, N. P., M. S. Fleming, and A. J. Horne. 2002. Denitrification Potential and Carbon Quality of Four Aquatic Plants in Wetland Microcosms. Soil Sci. Soc. Am. J. **66**: 1706–1712. doi:10.2136/sssaj2002.1706
Jacobs, S., W. Vandenbruwaene, K. Wolfstein, T. Maris, and S. Saathoff. 2013. Ecosystem Service Assessment of TIDE Estuaries. 90.
Jickells, T. D., and J. E. Rae. 2005. Biogeochemistry of intertidal sediments, Cambridge University Press.
Jones, C. M., D. R. H. Graf, D. Bru, L. Philippot, and S. Hallin. 2013. The unaccounted yet abundant nitrous oxide-reducing microbial community: A potential nitrous oxide sink. ISME J. **7**: 417–426. doi:10.1038/ismej.2012.125
Kawaida, S., K. Nanjo, N. Ohtsuchi, H. Kohno, and M. Sano. 2019. Cellulose digestion abilities determine the food utilization of mangrove estuarine crabs. Estuar. Coast. Shelf Sci. **222**: 43–52. doi:10.1016/j.ecss.2019.04.004
Kuenen, J. G. 2008. Anammox bacteria: From discovery to application. Nat. Rev. Microbiol. **6**: 320–326. doi:10.1038/nrmicro1857
Kuypers, M. M. M., H. K. Marchant, and B. Kartal. 2018. The microbial nitrogen-cycling network. Nat. Rev. Microbiol. **16**: 263–276. doi:10.1038/nrmicro.2018.9
Laverman, A. M., P. Van Cappellen, D. Van Rotterdam-Los, C. Pallud, and J. Abell. 2006. Potential rates and pathways of microbial nitrate reduction in coastal sediments. FEMS Microbiol. Ecol. **58**: 179–192. doi:10.1111/j.1574-6941.2006.00155.x
Laverman, A. M., T. Cazier, C. Yan, C. Roose-Amsaleg, F. Petit, J. Garnier, and T. Berthe. 2015. Exposure to vancomycin causes a shift in the microbial community structure without affecting nitrate reduction rates in river sediments. Environ. Sci. Pollut. Res. **22**: 13702–13709. doi:10.1007/s11356-015-4159-6
Laverman, A. M., J. Morelle, C. Roose-Amsaleg, and A. Pannard. 2021. Estuarine benthic nitrate reduction rates: Potential role of microalgae? Estuar. Coast. Shelf Sci. doi:https://doi.org/10.1016/j.ecss.2021.107394
Laverman, A. M., C. Pallud, J. Abell, and P. Van Cappellen. 2012. Comparative survey of potential nitrate and sulfate reduction rates in aquatic sediments. Geochim. Cosmochim. Acta **77**: 474–488.

doi:10.1016/j.gca.2011.10.033
Lee, I. O., J. Noh, J. Lee, and others. 2021. Stable isotope signatures reveal the significant contributions of microphytobenthos and saltmarsh-driven nutrition in the intertidal benthic food webs. Sci. Total Environ. **756**: 144068. doi:10.1016/j.scitotenv.2020.144068
Lee, J. A., and C. A. Francis. 2017. Spatiotemporal Characterization of San Francisco Bay Denitrifying Communities: a Comparison of nirK and nirS Diversity and Abundance. Microb. Ecol. **73**: 271–284. doi:10.1007/s00248-016-0865-y
Lemley, D. A., G. C. Snow, and L. R. D. Human. 2014. The decomposition of estuarine macrophytes under different temperature regimes. Water SA **40**: 117–124.
Lesourd, S., P. Lesueur, J. C. Brun-Cottan, J. P. Auffret, N. Poupinet, and B. Laignel. 2001. Morphosedimentary evolution of the macrotidal Seine estuary subjected to human impact. Estuaries **24**: 940–949. doi:10.2307/1353008
Lesourd, S., P. Lesueur, C. Fisson, and J. Dauvin. 2016. Sediment evolution in the mouth of the Seine estuary (France): A long-term monitoring during the last 150 years. C.R. Geosci. **348**: 442–450. doi:10.1016/j.crte.2015.08.001
Liu, Y., G. Villalba, R. U. Ayres, and H. Schroder. 2008. Global phosphorus flows and environmental impacts from a consumption perspective. J. Ind. Ecol. **12**: 229–247. doi:10.1111/j.1530-9290.2008.00025.x
Lorenzen, C. J. 1967. Determination of Chlorophyll and Pheo-Pigments : Spectrophotometric Equations. Limnol. Oceanogr. **12**: 343–346. doi:10.4319/lo.1967.12.2.0343
Magalhães, C. M., A. A. Bordalo, and W. J. Wiebe. 2002. Temporal and spatial patterns of intertidal sediment-water nutrient and oxygen fluxes in the Douro River estuary, Portugal. Mar. Ecol. Prog. Ser. **233**: 55–71. doi:10.3354/meps233055
Mandal, A., A. Dutta, R. Das, and J. Mukherjee. 2021. Role of intertidal microbial communities in carbon dioxide sequestration and pollutant removal: A review. Mar. Pollut. Bull. **170**: 112626. doi:10.1016/j.marpolbul.2021.112626
Mayor, D. J., B. Thornton, H. Jenkins, and S. L. Felgate. 2018. Microbiota: The Living Foundation, p. 43–61. *In* P.G. Beninger [ed.], Mudflat Ecology. Springer International Publishing.
McMillan, S. K., M. F. Piehler, S. P. Thompson, and H. W. Paerl. 2010. Denitrification of Nitrogen Released from Senescing Algal Biomass in Coastal Agricultural Headwater Streams. J. Environ. Qual. **39**: 274–281. doi:10.2134/jeq2008.0438
Le Moal, M., C. Gascuel-Odoux, A. Ménesguen, and others. 2019. Eutrophication: A new wine in an old bottle? Sci. Total Environ. **651**: 1–11. doi:10.1016/j.scitotenv.2018.09.139
Morelle, J. 2020. Projet SPORES : Synthèse sur les nutriments et la production primaire dans l'estuaire de la Seine.
Morelle, J., P. Claquin, and F. Orvain. 2020. Evidence for better microphytobenthos dynamics in mixed sand/mud zones than in pure sand or mud intertidal flats (Seine estuary, Normandy, France). PLoS One **15**: e0237211. doi:10.1371/journal.pone.0237211
Morelle, J., M. Schapira, F. Orvain, and others. 2018. Annual Phytoplankton Primary Production Estimation in a Temperate Estuary by Coupling PAM and Carbon Incorporation Methods. Estuaries and Coasts 1–19. doi:10.1007/s12237-018-0369-8
Nielsen, S. L., G. T. Banta, and M. F. Pedersen. 2004. Decomposition of marine primary producers: consequences for nutrient recycling and retention in coastal ecosystems, p. 187–216. *In* Estuarine nutrient cycling: the influence of primary producers. Springer.
Orvain, F., M. De Crignis, K. Guizien, S. Lefebvre, C. Mallet, E. Takahashi, and C. Dupuy. 2014. Tidal and seasonal effects on the short-term temporal patterns of bacteria, microphytobenthos and exopolymers in natural intertidal biofilms (Brouage, France). J. Sea Res.
Papaspyrou, S., C. J. Smith, L. F. Dong, C. Whitby, A. J. Dumbrell, and D. B. Nedwell. 2014. Nitrate reduction functional genes and nitrate reduction potentials persist in deeper estuarine sediments why? PLoS One **9**. doi:10.1371/journal.pone.0094111
Passarelli, C., C. Hubas, and D. M. Paterson. 2018. Mudflat Ecosystem Engineers and Services, p. 243–269. *In* Mudflat Ecology. Springer.
Philippot, L., A. Spor, C. Hénault, D. Bru, F. Bizouard, C. M. Jones, A. Sarr, and P. A. Maron. 2013. Loss in microbial diversity affects nitrogen cycling in soil. ISME J. **7**: 1609–1619. doi:10.1038/ismej.2013.34

753 Porter, E. M., W. D. Bowman, C. M. Clark, J. E. Compton, L. H. Pardo, and J. L. Soong. 2013.
754 Interactive effects of anthropogenic nitrogen enrichment and climate change on terrestrial and
755 aquatic biodiversity. Biogeochemistry **114**: 93–120. doi:10.1007/s10533-012-9803-3
756 Rich, J. J., R. S. Heichen, P. J. Bottomley, K. Cromack, and D. D. Myrold. 2003. Community
757 Composition and Functioning of Denitrifying Bacteria from Adjacent Meadow and Forest Soils.
758 Appl. Environ. Microbiol. **69**: 5974–5982. doi:10.1128/AEM.69.10.5974-5982.2003
759 Rösch, C., and H. Bothe. 2009. Diversity of total, nitrogen-fixing and denitrifying bacteria in an acid
760 forest soil. Eur. J. Soil Sci. **60**: 883–894. doi:10.1111/j.1365-2389.2009.01167.x
761 Scala, D. J., and L. J. Kerkhof. 1998. Nitrous oxide reductase (nosZ) gene-specific PCR primers for
762 detection of denitrifiers and three nosZ genes from marine sediments. FEMS Microbiol. Lett. **162**:
763 61–68. doi:10.1016/S0378-1097(98)00103-7
764 Semenov, M., E. Blagodatskaya, A. Stepanov, and Y. Kuzyakov. 2018. DNA-based determination of
765 soil microbial biomass in alkaline and carbonaceous soils of semi-arid climate. J. Arid Environ.
766 **150**: 54–61. doi:10.1016/j.jaridenv.2017.11.013
767 Shnyukova, E. I., and E. K. Zolotareva. 2017. Ecological Role of Exopolysaccharides of
768 Bacillariophyta : A Review. Int. J. Algae **19**: 5–24.
769 Sirivedhin, T., and K. A. Gray. 2006. Factors affecting denitrification rates in experimental wetlands:
770 Field and laboratory studies. Ecol. Eng. **26**: 167–181. doi:10.1016/j.ecoleng.2005.09.001
771 Smith, C. J., D. B. Nedwell, L. F. Dong, and A. M. Osborn. 2007. Diversity and abundance of nitrate
772 reductase genes (narG and napA), nitrite reductase genes (nirS and nrfA), and their transcripts in
773 estuarine sediments. Appl. Environ. Microbiol. **73**: 3612–3622. doi:10.1128/AEM.02894-06
774 Soares, M., and J. Rousk. 2019. Microbial growth and carbon use efficiency in soil: Links to fungal-
775 bacterial dominance, SOC-quality and stoichiometry. Soil Biol. Biochem. **131**: 195–205.
776 doi:10.1016/j.soilbio.2019.01.010
777 Starr, R. C., and R. W. Gillham. 1993. Denitrification and Organic Carbon Availability in Two Aquifers.
778 Groundwater **31**: 934–947. doi:10.1111/j.1745-6584.1993.tb00867.x
779 Stelzer, R. S., J. T. Scott, L. A. Bartsch, and T. B. Parr. 2014. Particulate organic matter quality
780 influences nitrate retention and denitrification in stream sediments: evidence from a carbon burial
781 experiment. Biogeochemistry **119**: 387–402. doi:10.1007/sl
782 Strous, M., J. G. Kuenen, and M. S. M. Jetten. 1999. Key physiology of anaerobic ammonium oxidation.
783 Appl. Environ. Microbiol. **65**: 3248–3250. doi:10.1128/aem.65.7.3248-3250.1999
784 Sundbäck, K., and A. Miles. 2002. Role of microphytobenthos and denitrification for nutrient turnover
785 in embayments with floating macroalgal mats: A spring situation. Aquat. Microb. Ecol. **30**: 91–
786 101. doi:10.3354/ame030091
787 Sundh, I. 1992. Biochemical composition of dissolved organic carbon derived from phytoplankton and
788 used by heterotrophic bacteria. Appl. Environ. Microbiol. **58**: 2938–2947.
789 doi:10.1128/aem.58.9.2938-2947.1992
790 Taylor, J. D., B. A. McKew, A. Kuhl, T. J. McGenity, and G. J. C. Underwood. 2013. Microphytobenthic
791 extracellular polymeric substances (EPS) in intertidal sediments fuel both generalist specialist
792 EPS-degrading bacteria. Limnol. Oceanogr. **58**: 1463–1480. doi:10.4319/lo.2013.58.4.1463
793 Tiedje, J. M. 1988. Ecology of denitrification and dissimilatory nitrate reduction to ammonium. Environ.
794 Microbiol. Anaerobes 179–244.
795 Tiedje, J. M., A. J. Sexstone, D. D. Myrold, and J. A. Robinson. 1983. Denitrification: ecological niches,
796 competition and survival. Antonie Van Leeuwenhoek **48**: 569–583. doi:10.1007/BF00399542
797 Tobias, C., A. Giblin, J. McClelland, J. Tucker, and B. Peterson. 2003. Sediment DIN fluxes and
798 preferential recycling of benthic microalgal nitrogen in a shallow macrotidal estuary. Mar. Ecol.
799 Prog. Ser. **257**: 25–36. doi:10.3354/meps257025
800 Trimmer, M., D. B. Nedwell, D. B. Sivyer, and S. J. Malcolm. 1998. Nitrogen fluxes through the lower
801 estuary of the river Great Ouse, England: The role of the bottom sediments. Mar. Ecol. Prog. Ser.
802 **163**: 109–124. doi:10.3354/meps163109
803 Ukaogo, P. O., U. Ewuzie, and C. V Onwuka. 2020. 21 - Environmental pollution: causes, effects, and
804 the remedies, p. 419–429. *In* P. Chowdhary, A. Raj, D. Verma, and Y. Akhter [eds.],
805 Microorganisms for Sustainable Environment and Health. Elsevier.
806 Underwood, G. J. C., and J. C. Kromkamp. 1999. Primary Production by Phytoplankton and
807 Microphytobenthos in Estuaries. Adv. Ecol. Res. **29**: 93–153. doi:10.1016/S0065-2504(08)60192-

0
Wadnerkar, P. D., I. R. Santos, A. Looman, C. J. Sanders, S. White, J. P. Tucker, and C. Holloway. 2019. Significant nitrate attenuation in a mangrove-fringed estuary during a flood-chase experiment. Environ. Pollut. **253**: 1000–1008. doi:10.1016/j.envpol.2019.06.060
Wang, J., Z. Chen, D. Wang, X. Sun, and S. Xu. 2009. Evaluation of dissolved inorganic nitrogen eliminating capability of the sediment in the tidal wetland of the Yangtze Estuary. J. Geogr. Sci. **19**: 447–460. doi:10.1007/s11442-009-0447-8
van der Wegen, M., B. Jaffe, A. Foxgrover, and D. Roelvink. 2017. Mudflat Morphodynamics and the Impact of Sea Level Rise in South San Francisco Bay. Estuaries and Coasts **40**: 37–49. doi:10.1007/s12237-016-0129-6
Wei, W., K. Isobe, T. Nishizawa, and others. 2015. Higher diversity and abundance of denitrifying microorganisms in environments than considered previously. ISME J. **9**: 1954–1965. doi:10.1038/ismej.2015.9
Welker, C., E. Sdrigotti, S. Covelli, and J. Faganeli. 2002. Microphytobenthos in the gulf of trieste (Northern Adriatic Sea): Relationship with labile sedimentary organic matter and nutrients. Estuar. Coast. Shelf Sci. **55**: 259–273. doi:10.1006/ecss.2001.0901
Zhang, X., Y. Zhang, P. Shi, Z. Bi, Z. Shan, and L. Ren. 2021. The deep challenge of nitrate pollution in river water of China. Sci. Total Environ. **770**: 144674. doi:10.1016/j.scitotenv.2020.144674
Zhou, S., S. Borjigin, S. Riya, A. Terada, and M. Hosomi. 2014. The relationship between anammox and denitrification in the sediment of an inland river. Sci. Total Environ. **490**: 1029–1036. doi:10.1016/j.scitotenv.2014.05.096
Zumft, W. G. 1997. Cell biology and molecular basis of denitrification. Microbiol. Mol. Biol. Rev. **61**: 533–616. doi:10.1128/.61.4.533-616.1997

Table 1. *Sediment characteristics before the FTR experiment and differences observed after the FTR experiment (357-h of incubation), for the unamended sediment (M0) and the 3 MPB amended sediments (M1, M5 and M10) all with a constant nitrogen supply (10 mM KNO_3). With the percentage of nitrogen (N) and carbon (C), the corresponding weight of carbon inside a reactor (g react^{-1}), the chlorophyll a and phaeopigment content (chl a and phaeo in µg gDSW^{-1}), and the EPS contents for low and high molecular weight carbohydrates and proteins (in µg gDSW^{-1}). The quantity of carbon per reactor was calculated considering the mean weight of 54.1g of sediment inside reactors*

	Elementary Analyses					**Photopigments (µg gDSW^{-1})**		**EPS (µg gDSW^{-1})**			
	N	C			C:N			Carbohydrates		Proteins	
	(%)	(%)	g react^{-1}	$\delta^{13}C$		Chl *a*	Phaeo	LMW	HMW	LMW	HMW
Sediment characteristics before experimentation											
M0	0.43	3.81	2.06	-25.5	10.3	5.7	12.9	255.0	147.1	5.5	11.5
M1	0.43	3.85	2.08	-25.6	10.4	8.1	31.5	260.0	154.6	5.7	11.6
M5	0.44	4.01	2.17	-24.8	10.6	17.2	39.1	279.8	184.9	6.3	11.9
M10	0.45	4.21	2.28	-24.0	10.9	28.6	48.6	304.5	222.8	7.1	12.2
Differences observed after the experiment											
M0	**-0.10** (-23%)	**-0.95** (-25%)	**0.51**	**-0.1** (-0.4%)	**-0.2** (-2.2%)	**-2.15** (-38%)	**+23.1** (+178%)	**-156.3** (-61%)	**-60.2** (-41%)	**+0.4** (+07%)	**-6.7** (-58%)
M1	**-0.08** (-19%)	**-0.71** (-18%)	**0.38**	**-0.1** (-0.4%)	**+0.0** (+0.2%)	**-2.38** (-29%)	**+4.1** (+13%)	**-173.3** (-67%)	**-53.6** (-35%)	**+1.7** (+30%)	**-7.4** (-64%)
M5	**-0.11** (-25%)	**-1.09** (-27%)	**0.59**	**-0.1** (-0.4%)	**-0.3** (-2.9%)	**-0.63** (-4%)	**+6.5** (+17%)	**-199.1** (-71%)	**-25.9** (-14%)	**+1.3** (+20%)	**-2.6** (-22%)
M10	**-0.07** (-16%)	**-0.90** (-21%)	**0.49**	**+0.3** (+1.3%)	**-0.7** (-6.9%)	**-6.39** (-22%)	**+18.5** (+38%)	**-217.3** (-71%)	**-51.3** (-23%)	**+2.1** (+30%)	**-5.2** (-42%)

Table 2. Average of the abundance of the microbial denitrifiers quantified via nir (±sd; n=12) and nosZ gene copies (±sd; n=6). *With the quantity of extracted DNA per ng of dry sediment, for the nir genes, the contributions of nirK and nirS and for nosZ genes, the contributions of the clades I & II nosZ.*

	µg ext. DNA gDSW^{-1}	**Nb of *nir* gene copies gDSW^{-1}**	**% of *nirK***	**% of *nirS***	**Nb of *nosZ* gene copies gDSW^{-1}**	**% of Clade I *nosZ***	**% of Clade II *nosZ***
IS	4.3	$6.3\times10^{7} \pm 1.7\times10^{7}$	11.8	88.2	$3.7\times10^{9} \pm 0.6\times10^{9}$	73.4	26.6
M0	13.8	$6.2\times10^{9} \pm 3.2\times10^{9}$	6.6	93.4	$30.9\times10^{9} \pm 1.3\times10^{9}$	77.9	22.1
M1	15.8	$9.5\times10^{9} \pm 3.1\times10^{9}$	5.6	94.4	$27.3\times10^{9} \pm 2.7\times10^{9}$	80.6	19.4
M5	19.3	$12.5\times10^{9} \pm 4.0\times10^{9}$	2.7	97.3	$28.0\times10^{9} \pm 5.5\times10^{9}$	82.6	17.4
M10	18.6	$16.2\times10^{9} \pm 7.0\times10^{9}$	1.6	98.4	$34.3\times10^{9} \pm 5.1\times10^{9}$	87.2	12.8

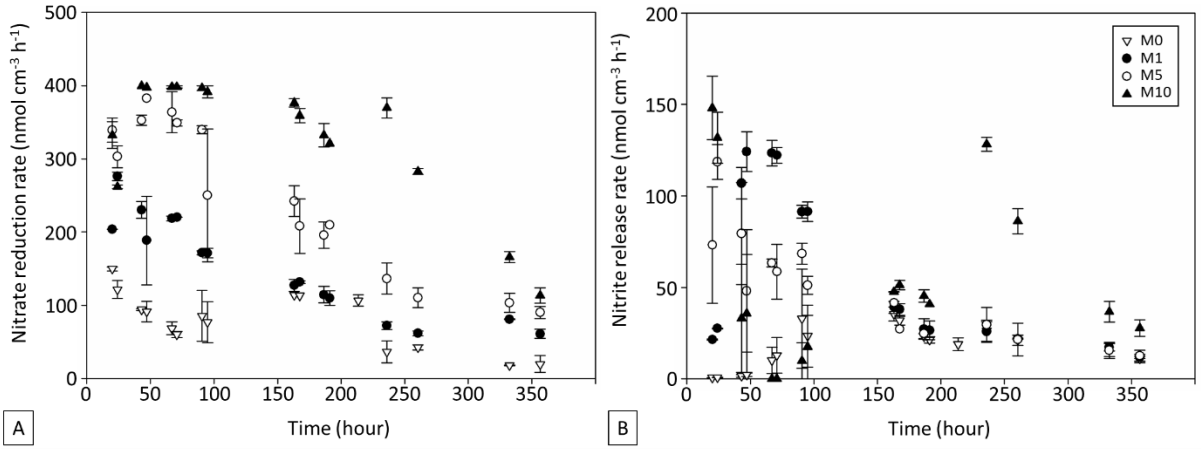

Figure 1. *Average (A) nitrate reduction rates and (B) nitrite release rates along the 357 hours of incubation (n=2) for the unamended sediment (M0) and the 3 MPB amended sediments (M1, M5 and M10) all with a constant nitrate supply (10 mM KNO_3).*

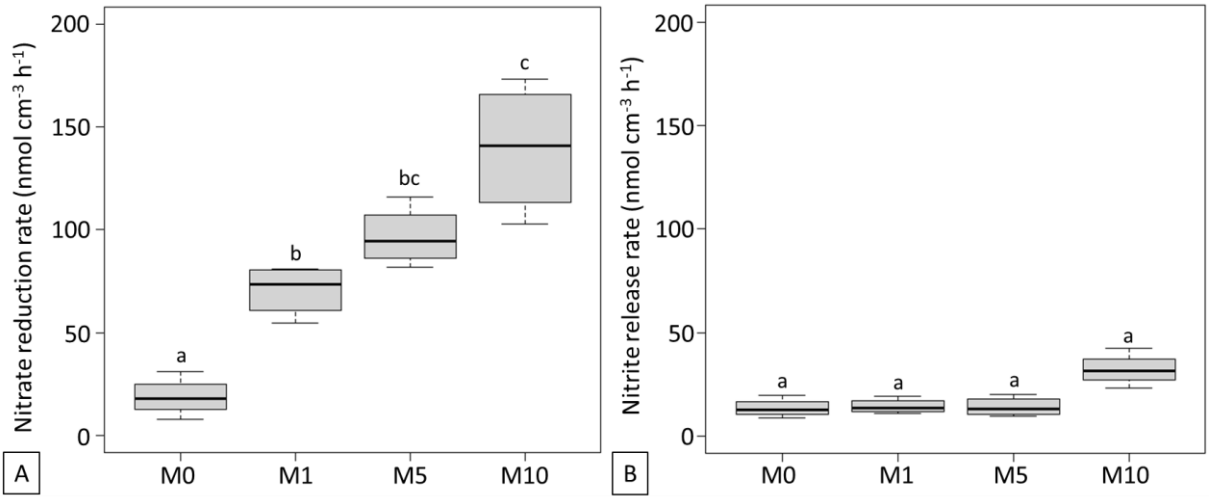

Figure 2. *A. Boxplot of nitrate reduction rates (A) and nitrite release rates (B) at the end of the experiment (332- 356 hours; n=4) for the unamended sediment (M0) and the 3 MPB amended sediments (M1, M5 and M10) all with a constant nitrate supply (10 mM KNO_3). The letters above the boxes correspond to the statistical results of an anova followed by a post-hoc test; a different letter represents a significant difference between treatments.*

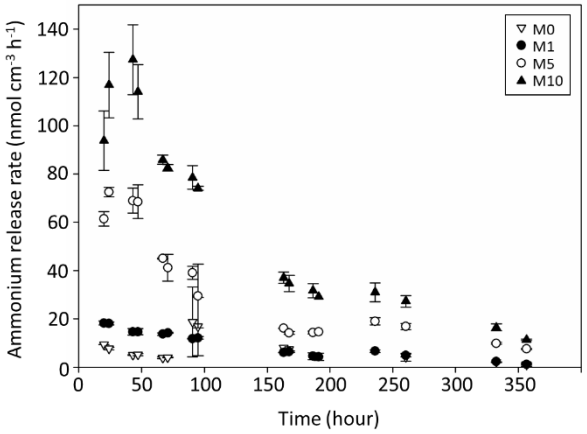

Figure 3. *Average ammonium release rates along the 357 hours of incubation (n=2), for the unamended sediment (M0) and the 3 MPB amended sediments (M1, M5 and M10) all with a constant nitrate supply (10 mM KNO_3).*

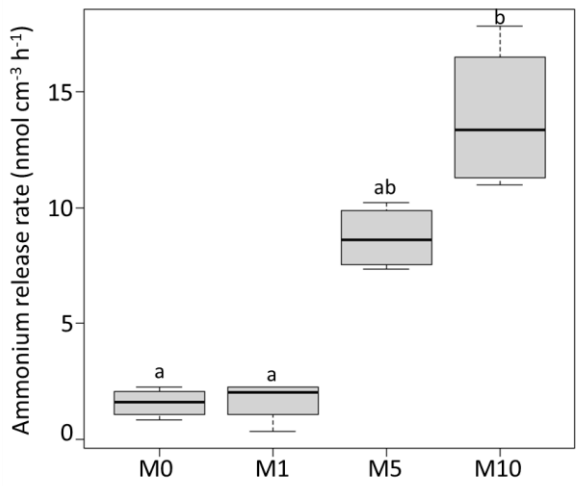

Figure 4. *Average ammonium release rates at the end of the experiment (332- 356 hours; n=4), for the unamended sediment (M0) and the 3 MPB amended sediments (M1, M5 and M10) all with a constant nitrate supply (10 mM KNO_3).*

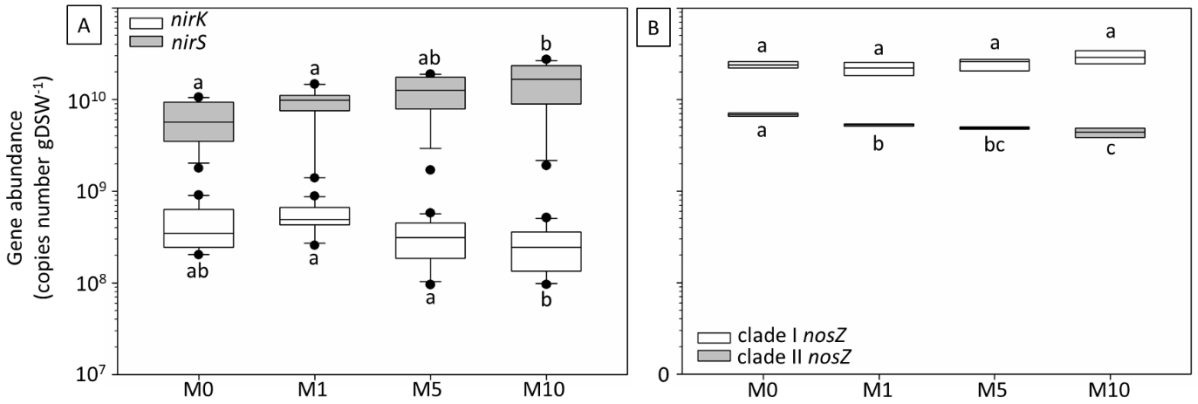

Figure 5. Denitrification genes abundance *for (A) the nir genes (nirK in white and nirS in grey; n=12) encoding the reduction of nitrite to nitric oxide and (B) The nosZ genes (nosZ clade I in white and nosZ Clade II in grey, n=6) encoding the nitrous oxide reductase, for the unamended sediment (M0) and the 3 MPB amended sediments (M1, M5 and M10) all with a constant nitrogen supply (10 mM KNO_3).*

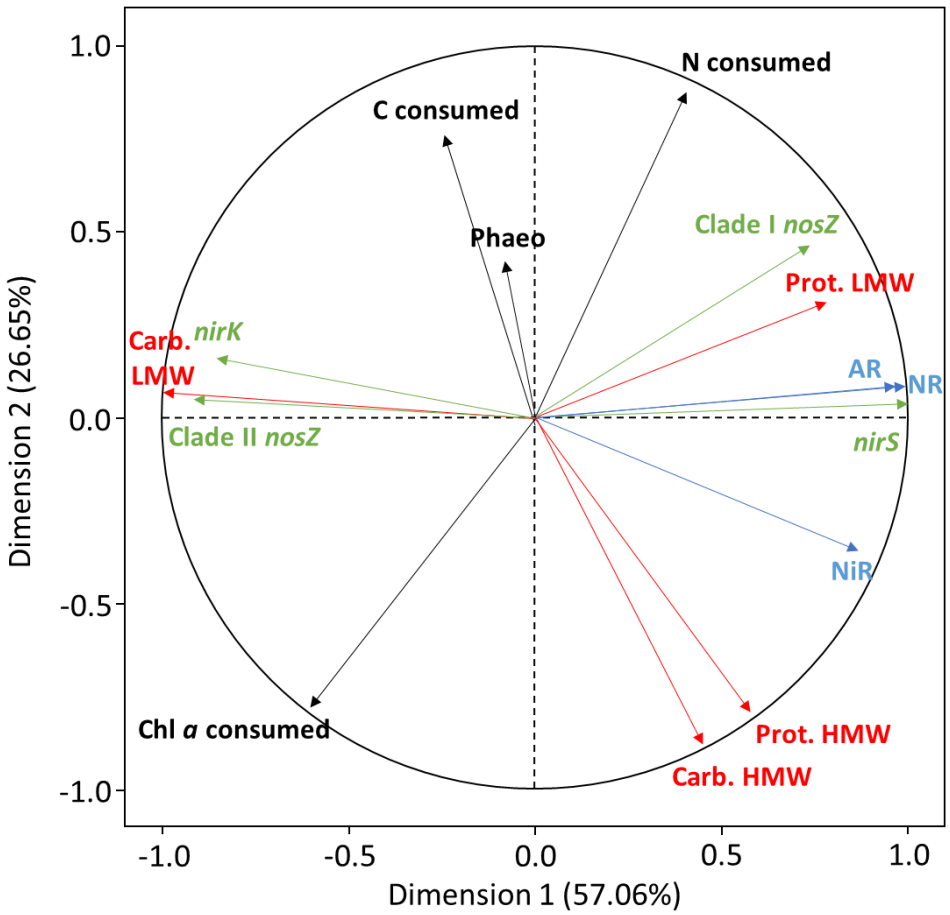

Figure 6. *A. Principal component analyse (PCA) on values representing the differences between before and after incubation in the FTR (table 2). With the percentage of nitrogen (N) and carbon (C) consumed, the quantity of phaeopigment produced (Phaeo); the quantity of chlorophyll a (Chl a), and EPS consumed (Carb. HMW; Carb. LMW; Prot. HMW) or produced (Prot. LMW); the microbial denitrifying communities (difference in relative abundance of nirK, nirS and nosZ clade 1&2); the quantity of nitrate consumed (NR), and the quantities of nitrite and ammonium released (NiR and AR respectively).*